Biomaterials Science

ROYAL SOCIETY OF CHEMISTRY

PAPER

View Article Online
View Journal | View Issue

Check for updates

Cite this: *Biomater. Sci.*, 2022, **10**, 2224

Molecular weight tuning optimizes poly(2-methoxyethyl acrylate) dispersion to enhance the aging resistance and anti-fouling behavior of denture base resin†

Jie Jin,[a] Rajani Bhat,[b] Utkarsh Mangal,[a] Ji-Young Seo,[a] YouJin Min,[c] Jaehun Yu,[a,d] Dae-Eun Kim,[c] Kenichi Kuroda,*[b] Jae-Sung Kwon*[d,e] and Sung-Hwan Choi*[a,d]

Poly(methyl methacrylate) (PMMA)-based denture base resins easily develop oral bacterial and fungal biofilms, which may constitute a significant health risk. Conventional bacterial-resistant additives and coatings often cause undesirable changes in the resin. Reduced bacterial resistance over time in the harsh oral environment is a major challenge in resin development. Poly(2-methoxyethyl acrylate) (PMEA) has anti-fouling properties; however, due to the oily/rubbery state of this polymer, and its surface aggregation tendency in a resin mixture, its direct use as a resin additive is limited. This study aimed to optimize the use of PMEA in dental resins. Acrylic resins containing a series of PMEA polymers with various molecular weights (MWs) at different concentrations were prepared, and the mechanical properties, surface gloss, direct transmittance, and cytotoxicity were evaluated, along with the distribution of PMEA in the resin. Resins with low-MW PMEA (2000 g mol^{-1}) (PMEA-1) at low concentrations satisfied the clinical requirements for denture resins, and the PMEA was homogeneously distributed. The anti-fouling performance of the resin was evaluated for protein adsorption, bacterial and fungal attachment, and saliva-derived biofilm formation. The PMEA-1 resin most effectively inhibited biofilm formation (~50% reduction in biofilm mass and thickness compared to those of the control). Post-aged resins maintained their mechanical properties and anti-fouling activity, and polished surfaces had the same anti-biofilm behavior. Based on wettability and tribological results, we propose that the PMEA additive creates a non-stick surface to inhibit biofilm formation. This study demonstrated that PMEA additives can provide a stable and biocompatible anti-fouling surface, without sacrificing the mechanical properties and aesthetics of denture resins.

Received 12th January 2022,
Accepted 10th March 2022

DOI: 10.1039/d2bm00053a

rsc.li/biomaterials-science

Introduction

According to the American College of Prosthodontics, more than 36 million Americans are edentulous, and 90% of edentulous adults wear dentures. The use of dentures is projected to become more important in the future. However, the typical poly(methyl methacrylate) (PMMA)-based denture base acrylic resins are prone to the formation of oral bacterial and fungal biofilms,[1–7] which often pose a significant health risk.[8–10] The resin–oral-tissue interface tends to accumulate oral bacteria and fungi, leading to biofilm formation, which may cause oral stomatitis and severe infections. In particular, denture stomatitis affects 15–70% of denture wearers.[11,12]

Much effort has been dedicated to the development of anti-fouling dental resins; however, significant limitations persist in their performance and processing. Surface covalent modification with anti-fouling polymers, *e.g.*, polymer chains that form brush-like structures, is a promising technique.[13–15]

[a]*Department of Orthodontics, Institute of Craniofacial Deformity, Yonsei University College of Dentistry, 50-1 Yonsei-ro, Seodaemun-gu, Seoul 03722, Republic of Korea. E-mail: selfexam@yuhs.ac*
[b]*Department of Biologic & Materials Sciences & Prosthodontics, University of Michigan School of Dentistry, 1011 N. University Ave., Ann Arbor, MI 48109, USA*
[c]*Department of Mechanical Engineering, Yonsei University, Seoul, 03722, Republic of Korea*
[d]*BK21 FOUR Project, Yonsei University College of Dentistry, 50-1 Yonsei-ro, Seodaemun-gu, Seoul 03722, Republic of Korea. E-mail: jkwon@yuhs.ac, kkuroda@umich.edu*
[e]*Department and Research Institute of Dental Biomaterials and Bioengineering, Yonsei University College of Dentistry, 50-1 Yonsei-ro, Seodaemun-gu, Seoul 03722, Republic of Korea*

† Electronic supplementary information (ESI) available. See DOI: https://doi.org/10.1039/d2bm00053a

However, the denture surface is subject to constant abrasion and scratching during use and cleaning; this may cause coating failure and require frequent replenishment. Surface modification also needs to use harsh chemical conditions and additional processing steps.

Alternatively, the incorporation of anti-fouling ionic monomers into resins, such as zwitterionic monomers, has also yielded excellent anti-fouling performance. These anti-fouling additives were added to conventional resins during polymerization; thus, this approach is more practical and suitable for denture fabrication than post-polymerization surface modifications. Because scratched surfaces can expose anti-fouling agents in the matrix, the dentures maintain resistance to fouling during use. However, these additives can degrade the mechanical properties and aesthetics of resins because of the inherent immiscibility of ionic monomers in hydrophobic monomers and resins.[16,17] Thus, there are trade-offs between clinical anti-fouling performance, mechanical and aesthetic properties, and processing practicality, which pose significant limitations on the clinical implementation of anti-fouling dental resins.

To address this problem, we designed a straightforward strategy that enables the use of a polymer additive for anti-fouling denture base resins. This strategy exploits the inherent anti-fouling activity and physicochemical properties of poly(2-methoxyethyl acrylate) (PMEA) as a polymer additive. As a biocompatible material approved by the U.S. Food and Drug Administration, the primary application of PMEA has been to improve blood compatibility as a material for medical device anti-fouling coatings.[18–20] In addition, there are some studies of PMEA polymer films in mixtures with PMMA that showed low protein adhesion to their surfaces.[21–23] Although it has anti-fouling activity, PMEA is water immiscible, but miscible with acrylic monomers; this characteristic could minimize the degradation of the mechanical properties of dental resins. PMEA is relatively hydrophobic, which contrasts with traditional anti-fouling polymers such as water-soluble PEG and zwitterionic polymers. Hence, PMEA would not leach out to the oral aqueous environment and provide stable anti-fouling surfaces, while it is not covalently incorporated in the resin. Therefore, PMEA is considered a potential polymer additive to develop anti-fouling denture base resins, which can extend the applicability of PMEA in biomedical fields.

Although PMEA is known for its potent anti-fouling activity,[24] its clinical application has been challenging. Because of its oily/rubbery state, the use of PMEA in high contents has been limited to low-mechanical-load applications. In addition, it has been previously demonstrated that PMEA migrates to the surface of PMMA films after annealing,[25] which is not ideal for dental resins that require the polishing of the resin surface in the standard fabrication process.

In this study, PMEA samples with different molecular weight (MW) were synthesized for use. It has been reported that the MW of PMEA determines the entanglement, and hence, mobility of polymer chains.[26] Considering that the conventional method of preparing PMMA films is different from that of dental resin, it is necessary to study the distribution of PMEA in bulk resin, and the effects of different MWs and contents of PMEA on the mechanical properties of dental resins. In addition, the fibrinogen and platelet attachment on PMEA coatings has been extensively investigated.[26,27] However, there are few studies on microbial attachment and biofilm formation.[28] Therefore, when MW-tuned PMEA was used as an additive for dental resins, it was hypothesized that: (1) the specific MW and content of PMEA would not affect the mechanical properties of the resin; (2) PMEA would homogeneously distribute in the PMMA bulk polymer; and (3) PMEA would prevent oral bacterial attachment and biofilm formation on the resin surfaces.

To test these hypotheses and achieve the goal of developing anti-fouling dental resin, commercial denture base acrylic resins were synthesized with the addition of PMEA. The bulk mechanical properties and appearance of these resins were examined to identify the resin compositions optimal for clinical applications. The anti-fouling activity of these resins against bovine serum albumin (BSA) and oral microbes was evaluated. To assess the clinical durability and stability of the resins, the resins were aged by thermocycling or long-term exposure to water, and their mechanical properties and anti-fouling performance were evaluated. The resin surfaces were also polished to simulate abrasion due to contact with food and oral tissue, brushing, and the denture fabrication process, and their anti-biofilm activity against oral bacteria was evaluated.

Experimental

Materials

An auto-polymerizing orthodontic acrylic resin was purchased from Ortho-Jet, Lang Dental Manufacturing Co. Inc. (Chicago, Ill, USA). Thiazolyl blue tetrazolium bromide, isoamyl acetate, 2,2′-azobisisobutyronitrile (AIBN) and 2-methoxyethyl acrylate (MEA) were purchased from Sigma-Aldrich (St Louis, MO, USA). Methyl mercaptopropionate (MMP) and reagent-grade solvents were purchased from Fisher Scientific (Waltham, MA, USA). Methacryloyl thiocarbamoyl Rhodamine-B (RhB) was purchased from Polysciences (Washington, PA, USA). Prior to polymerization, MEA monomer was passed through an alumina column to remove the inhibitor. AIBN was recrystallized with hot methanol, prior to use. Other chemicals were used as received without further purification. PBS was purchased from Welgene (Gyeongsan, Gyeongsangbuk-do, Korea). BSA and micro-bicinchoninic acid (Micro BCATM Protein Assay Kit) were purchased from Pierce Biotechnology (Rockford, IL, USA). Dulbecco's modified Eagle's medium was obtained from Gibco BRL (Gaithersburg, MD, USA) and used as a cell culture medium. LIVE/DEAD bacterial viability kits were purchased from Molecular Probes (Eugene, OR, USA).

Instruments

Gel permeation chromatography (GPC) analysis was performed using a Waters 1515 HPLC instrument (Waters Co., Milford,

MA, USA) equipped with Waters Styragel (7.8 mm × 300 mm) HR 0.5, HR 1, and HR 4 columns in sequence and detected by a differential refractometer (RI) using PMMA standards. ^{1}H NMR spectroscopy was performed using a Varian MR400 (400 MHz) (Varian, Inc., Palo Alto, CA, USA) and Bruker 600 NMR (Bruker Daltonics, Bremen, Germany), and the data was analyzed using MestReNova software (Mestrelab Research SL, Spain). Thermocycling aging was conducted using a Thermal Cyclic Tester (R&B Inc., Daejeon, Korea). Flexural strength and elastic modulus were evaluated with a universal testing machine (Model 3366, Instron, Norwood, MA, USA). A hardness tester (DMH-2, Matsuzawa Seiki Co. Ltd, Akita-shi, Japan) was used for determining the Vickers hardness. An infrared gloss meter (IG-330, Horiba, Kyoto, Japan) was used to measure the surface gloss. Direct transmittance (T%) was measured using an ultraviolet-visible (UV/vis) spectrophotometer (Lambda 20, PerkinElmer, Waltham, MA, USA). Static contact angle, surface energy, and contact angle hysteresis of liquids on surfaces were measured using a contact angle analyzer (SmartDrop Lab, Femtobiomed Inc., Seongnam, South Korea). An ion coater (ACE600; Leica, Wien, Austria) was used to coat samples with Pt before scanning electron microscopy (SEM) observation. Samples with bacteria and fungi were subjected to critical point drying (Leica EM CPD300; Leica, Wien, Austria) before SEM. SEM images were observed *via* field emission SEM (FE-SEM; Merin, Carl Zeiss, Oberkochen, Germany). A Nikon Eclipse TE300 (Nikon, Melville, NY, USA) was used to evaluate the PMEA distribution in the resin and at the resin surface. A micro-plate reader (Epoch, BioTek Instruments, Winooski, VT, USA) was used to measure the sample absorbance. Confocal laser microscopy (CLSM; LSM880, Carl Zeiss, Thornwood, NY, USA) was used to observe fluorescence images of bacteria and biofilm. The biofilm thickness was measured using Zen software (Carl Zeiss Microscopy, LLC, Thornwood, NY, USA). The average biomass was measured using the COMSTAT plug-in (Technical University of Denmark) along with the ImageJ software (National Institutes of Health, NIH).

Polymer synthesis and characterization

We synthesized a series of PMEA with a range of MWs by free-radical polymerization in the presence of a thienyl chain transfer agent (CTA) to investigate the effect of MW on their properties (Scheme 1). In a round bottom flask, 2-methoxyethyl acrylate, methyl mercaptopropionate (MMP) and AIBN were dissolved in acetonitrile to give a monomer concentration of ~2 M. Table 1 shows the feed compositions. The reaction mixture was sealed and purged with nitrogen gas for 45 min and then was immersed in an oil bath at 70 °C. The reaction was allowed to stir at 70 °C for 16 h, after which the mixture was cooled in a dry ice/acetone bath to stop polymerization, and then the mixture was exposed to air. The solvent was evaporated, and the solution was added dropwise into rapidly stirred cold hexane. The hexane layer was decanted, and the viscous polymer was dissolved again in small amount of dichloromethane and was added dropwise into rapidly stirred cold hexane. The hexane layer was decanted, and the polymer was dried under vacuum for 24 h to yield a viscous polymer. Low-MW polymers were prepared by increasing the ratio of CTA to monomer. The samples synthesized with 10%, 1%, 0.1%, and 0% MMP were denoted as PMEA-1, PMEA-2, PMEA-3, and PMEA-4, respectively (Table 1). The polymer synthesis was repeated, and the different polymer lots are denoted as "a" and "b". The polymer series "a" was used for the mechanical properties test and morphological characterization observation. The polymer series "b" was used for other experiments.

Table 1 Feed composition and yield of PMEA synthesis

	MEA monomer (mol)	MMP (mol)	AIBN (mol)	Yield
PMEA-1	0.35	0.035	0.007	95%
PMEA-2	0.35	0.0035	0.0007	93%
PMEA-3	0.35	0.00035	0.00007	88%
PMEA-4	0.35	0	0.0035	85%
PMEA-1Rh (0.01 mol%)	0.35 (Rh = 35 μmol)	0.035	0.007	91%
PMMA-Rh	0.11 (Rh = 11 μmol)	0.011	0.002	85%

PMMA, poly(methyl methacrylate); MEA, 2-methoxyethyl acrylate; PMEA, poly(2-methoxyethyl acrylate); Rh, Rhodamine monomer.

The conversion and degree of polymerization (DP) were determined by ^{1}H NMR spectroscopy. The MW of the PMEA polymers was calculated using the DP and the NWs of the monomers and MMP (Table 2). The MW and its distribution were also determined by GPC. All the polymer samples were oily or viscous liquid.

The synthesis of rhodamine-labeled PMEA-1 (PMEA-1Rh) polymer was performed with the addition of methacryloyl thiocarbamoyl RhB monomer (0.01 mol%) in the same manner as described above. The details of the synthesis of PMMA-Rh polymer are described in ESI.†

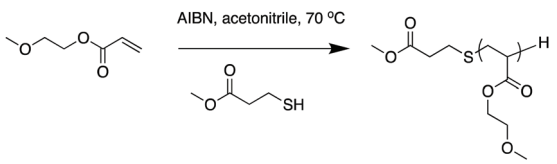

Scheme 1 Synthesis of poly(2-methoxyethyl acrylate) (PMEA) in the presence of methyl mercaptopropionate (MMP) as a chain transfer reagent.

Resin preparation

The PMEA polymers were dissolved in an MMA monomer at different PMEA concentrations by continuously stirring for 24 h. The MMA liquid containing the PMEA polymers was mixed with the PMMA powder in a mass ratio of 2 : 3, and the final concentration of PMEA was varied from 0 to 10 wt% (Table 3). The mixture was stirred for 15 s, and then poured into standardized polyacetal resin moulds (disc or bar shapes) and subjected to low-temperature polymerization (60 °C, 0.4

Table 2 Characterization of polymers

Series	Polymer	M_n NMR[a]	M_n GPC[b]	MW GPC[b]	$Đ_m$ [b]
a	PMEA-1	1700	1680	2200	1.3
	PMEA-2	8100	9900	19 000	1.9
	PMEA-3	38 000	59 200	164 000	2.8
	PMEA-4	—	83 000	400 000	5.0
b	PMEA-1	1200	1200	2000	1.6
	PMEA-4	—	116 000	412 000	3.5
Rh labeled	PMEA-1Rh	1270	1640	2300	1.4
	PMMA-Rh	4000	4200	6000	1.4

[a] Number average molecular weight (M_n) calculated using DP determined by ^{1}H NMR and molecular weights (MW) of monomers and MMP. [b] Molecular weight dispersity ($Đ_m$) determined by GPC (determined by PMMA standards).

Table 3 Compositions of the control and experimental groups

	Composition of PMMA, MMA, and PMEA (wt%)		
Composition fraction of PMEA	PMMA powder	MMA liquid	PMEA
0%	60.0	40.0	0
3%	58.2	38.8	3.0
5%	57.0	38.0	5.0
10%	54.0	36.0	10.0

PMMA, poly(methyl methacrylate); MMA, methyl methacrylate; PMEA, poly(2-methoxyethyl acrylate).

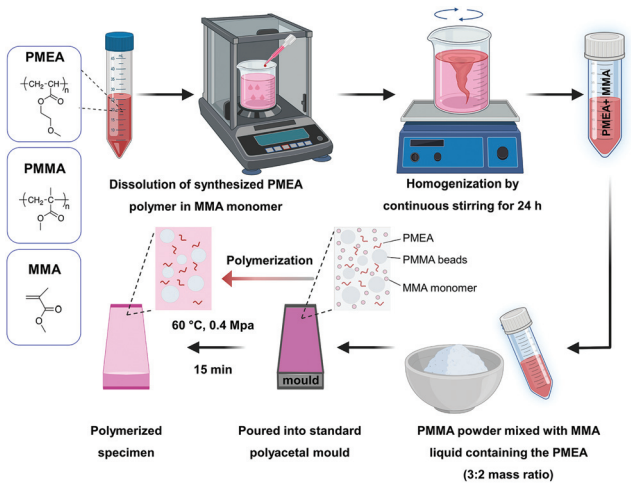

Fig. 1 Preparation of denture base resin with PMEA.

MPa) for 15 min (Fig. 1). The specimens were polished with SiC paper (up to 2000 grit) before testing their mechanical properties (flexural strength, elastic modulus, and Vickers hardness). Prior to experiments, all specimens were stored in distilled water at 37 °C for 48 h according to ISO standards.[29] It should be noted that the preparation of specimens with 10% PMEA-3 and 10% PMEA-4 was failed due to fast curing of the mixtures. For comparison, resins with monomer MEA was also prepared using the same procedure instead of PMEA. Bar-shaped specimens of 64 mm (length) × 10 mm (width) × 3.3 mm (height) were fabricated to evaluate the mechanical properties. The disc-shaped samples (diameter: 10 mm, thickness: 2 mm) were used for biological analysis. Prior to the biological experiments, the specimens were sterilized with ethylene oxide gas according to a previous study.[30,31]

Sample aging

Durability analyses were performed with resin specimens subject to thermocycling aging to evaluate the mechanical properties and static-immersion aging for evaluating the long-term anti-biofilm performance, based on our previous studies.[13,32] The specimens for long-term mechanical properties were subjected to thermocycling equipment (Thermal Cyclic Tester, R&B Inc.) set to a thermo-cycle of 45 s dwell time and 5 s transfer time for 850 cycles. Thermocycling simulates the periodic thermal fluctuations in the oral environment, with an estimate of ~10 000 cycles per year.[33] The resins underwent 850 cycles (5 to 55 °C), 45 s dwell time, and 5 s transfer time, which mimics the number of cycles for approximately one month in the mouth.[17] To evaluate the long-term anti-biofilm performance, the disc-shaped samples (diameter: 10 mm, thickness: 2 mm) were immersed in distilled water for seven days at 37 °C.

Mechanical testing

Bar-shaped specimens (n = 6) of 64 mm (length) × 10 mm (width) × 3.3 mm (height) were fabricated to evaluate the mechanical properties. The tests were performed following ISO 20795-2.[29] Three-point flexure tests were performed to evaluate the flexural strength and elastic modulus with a universal testing machine (Model 3366, Instron). The crosshead speed was 5 mm min^{-1}, and the span length was 50 mm. The formulas for flexural strength and elastic modulus were taken from ISO 20795-2.[29] A hardness tester (DMH-2) was used for determining the Vickers hardness. The tester was adjusted to a load of 300 gf (2.94 N) for 30 s. For each sample, the average value was calculated from three indentations.

Morphological characterization

To characterize the PMEA-PMMA specimens, bar-shaped samples with dimensions of 64 mm (length) × 10 mm (width) × 3.3 mm (height) were fractured by a computer-controlled universal testing machine. The fractured surfaces of the samples were coated with a 5 nm film of Pt using an ion coater (ACE600), and then imaged using FE-SEM at 5 kV.

Cytotoxicity tests

The 3-(4,5-dimethylthiazol-2-yl)-2,5-diphenyltetrazolium bromide (MTT) assay was used to measure cytotoxicity according to ISO 10993-5,[34] with an L929 experimental cell. The samples were soaked in cell culture medium (3 cm^2 ml^{-1}) at 37 °C for 24 h to prepare extractions in accordance with ISO 10993-12.[35] L929 cells (1 × 10^5) were cultured in an incubator

at 37 °C and 5% CO_2 for 24 h, and then the original culture medium was replaced by 100 μL per well of 100% extractions. After 24 h, the medium was replaced with 50 μL per well of thiazolyl blue tetrazolium bromide solution. Then replace the MTT solution with 100 μL per well of isopropanol and shake slightly for 30 min. A micro-plate reader (Epoch) was used to measure the absorbance at 570 nm.

PMEA distribution

The PMEA-Rh and PMMA-Rh polymers were stirred overnight with the liquid component of Ortho-Jet Lang dental resin. The liquid mixture (polymer and liquid component) was mixed with the solid component of the resin in a mass ratio of 2 : 3. The viscous mixture was stirred for 10 s and poured on to a glass slide and pressed with a coverslip. The resin was allowed to cure at room temperature for 2 h. The concentration of polymer in the final solid resin was 3 wt%. Confocal microscopy was performed using a Nikon Eclipse TE300 (Nikon). For Fig. 2A the specimen was cut vertically for exposing the cross-section with a thickness of 780 μm. It was then placed in a polypropylene mold and embedded in a clear PMMA resin to expose the cross-section. The entire disc was then polished to get a suitable surface for imaging. For Fig. 2B and C, the slide containing the specimen was placed directly on the stage of the inverted confocal scanning laser microscope. Z-stack imaging was performed to get a view of the distribution of rhodamine-labeled polymer in the entire resin.

Characterization of wettability

For wetting analysis, the contact angle, surface energy, and contact angle hysteresis of liquids on the resin surfaces were measured using a contact angle analyzer (SmartDrop). Disc-

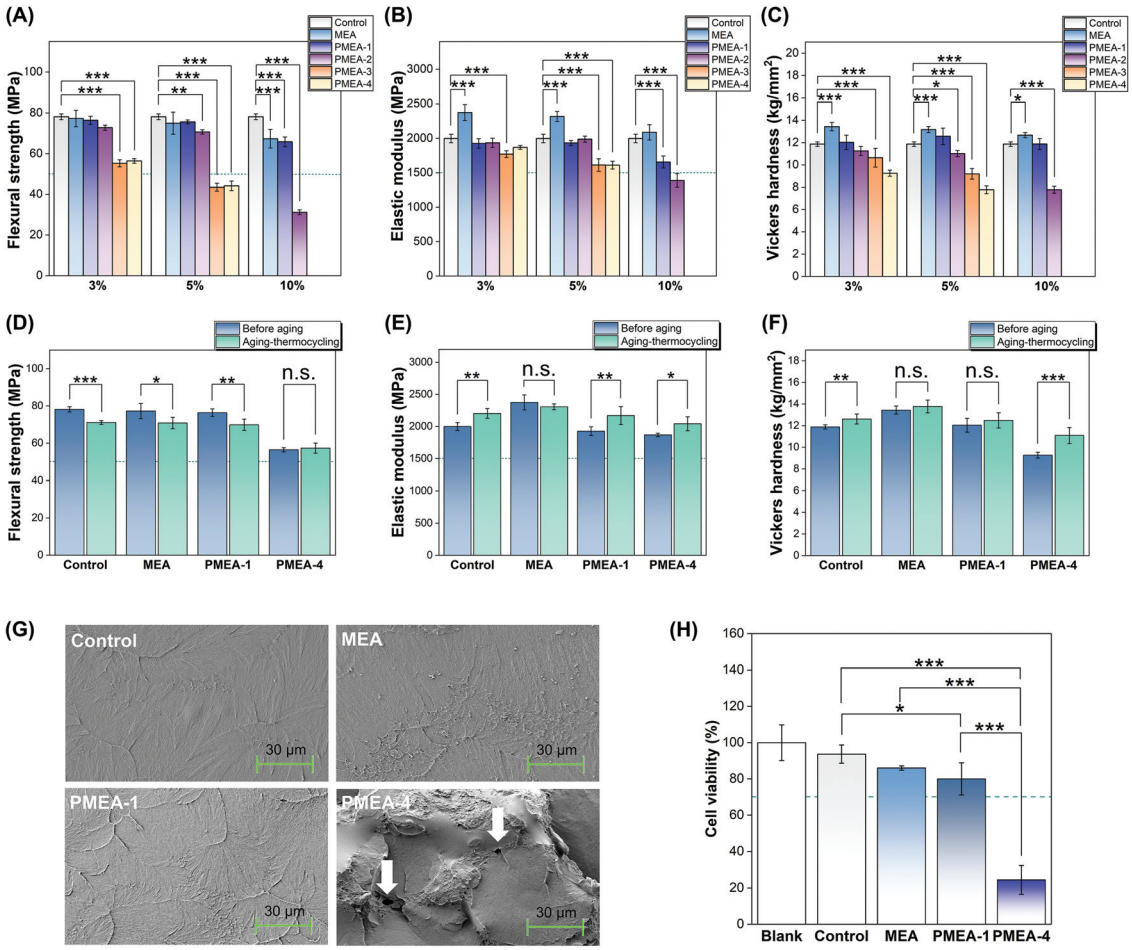

Fig. 2 Mechanical properties of resins with PMEA: (A) flexural strength, (B) elastic modulus, and (C) Vickers hardness of MEA resin, PMEA resins, and control (commercial resin). Asterisks indicate statistical significance compared to control (* $P < 0.05$, ** $P < 0.01$, and *** $P < 0.001$). (D) Flexural strength, (E) elastic modulus, and (F) Vickers hardness of pre- and post-thermocycled resins. Statistical differences are listed in Tables S4–6.† Asterisks indicate statistically significant change due to thermocycling (n.s.: not significant, * $P < 0.05$, ** $P < 0.01$, and *** $P < 0.001$). Dashed lines in (A), (B), (D), and (E) indicate the minimum required mechanical strength according to ISO 20795-2. (G) SEM images of fractured resin surfaces (1000× magnification). White arrows indicate pores. (H) Cell viability (%) of L929 cells exposed to the extraction of resin. Dashed lines in panels indicates the minimum required cell viability in accordance with ISO 10993-5. Asterisks indicate statistical significance (* $P < 0.05$, ** $P < 0.01$, and *** $P < 0.001$). The PMEA polymer series "a" was used for mechanical testing and morphological characterization, and the PMEA polymer series "b" was used for the cytotoxicity test (Table 2).

shaped samples (n = 5) were fabricated. Distilled water and 2 mg ml^{-1} BSA were chosen as the reference liquids. To confirm the reproducibility of the measurements, the tests were conducted at three different positions on each sample. The surface energy was calculated using the software of the analyzer, and the calculation was based on the Bashforth–Adams equation which describes the gravity-driven droplet distortion of a reference solution, and Young's equation which describes the relationship between the contact angle and surface energy.

Tribological performance

The tribological performance was assessed using a reciprocating-type tribometer under a normal load of 50 mN at a speed of 2 mm s^{-1} (0.5 Hz) for 1000 sliding cycles at 24 °C and relative humidity of 25–30%. PBS (10 mL) was dropped using a micropipette for lubrication. As the counter surface, a 304 stainless steel ball with a diameter of 5 mm was used. Each test was repeated at least three times to ensure the reliability of the experimental data.

Bacterial and fungal attachment

The fungal and bacterial attachment to the resin surface was evaluated in accordance with previously established methods.[36–39] *Candida albicans* (*C. albicans*) [Korean Collection for Oral Microbiology (KCOM) 1301] and *Streptococcus mutans* (*S. mutans*) (ATCC 25175) were selected as representatives of fungi and bacteria, respectively. The fungal or bacterial suspension (1 mL, 1×10^7 cells per mL for *C. albicans* and 1×10^8 cells per mL for *S. mutans*) was dropped onto samples (disc-shaped, diameter: 10 mm, thickness: 2 mm) and then incubated at 37 °C for 24 h. After incubation, the samples were washed twice with PBS to remove non-adherent fungi or bacteria. The bacteria adhering to the sample surface were harvested by sonication for 5 min. The samples were soaked in bacterial or fungal suspension and then incubated at 37 °C for 24 h. Subsequently, the suspension was diluted with different concentrations, and spread (100 μL) on an agar plate, followed by culturing at 37 °C in an incubator for 24 h to determine the total number of bacterial colony-forming units (CFUs).

The viability of the adherent bacteria was examined using a LIVE/DEAD bacterial viability kit (Molecular Probes). Bacteria were cultured in the same way as CFU determination. The stained samples were observed by CLSM (LSM880). Live bacteria appeared green while the dead bacteria appeared red.

For SEM analysis, the samples with adhered bacteria were fixed with 2% glutaraldehyde–paraformaldehyde in 0.1 M PBS for 30 min at room temperature. The samples were post-fixed with 1% OsO_4 dissolved in 0.1 M PBS for 2 h, dehydrated in an ascending gradual series of ethanol, treated with isoamyl acetate, and subjected to critical point drying (EM CPD300). Then, the discs were coated with 5 nm Pt using an ion coater (ACE600; Leica). They were then evaluated by FE-SEM at 7 kV.

Saliva-derived biofilm model and biomass measurements

Human-saliva-derived biofilm analyses were carried out according to previously established methods.[38,40] The saliva was obtained in accordance with the ethical principles of the 64th World Medical Association Declaration of Helsinki and the following procedures approved by the institutional review board of the Yonsei University Dental Hospital (Seoul, Republic of Korea) (2-2019-0049). Written informed consent was obtained from all participants before donating saliva. The human saliva obtained from six adults was mixed in equal proportions and then diluted to 30% in sterile glycerol and stored at −80 °C.

McBain medium was prepared according to previous studies to simulate the saliva environment for cultivating biofilm models.[40] The medium (1.5 mL) after 24 h of incubation with human saliva was dropped onto samples (diameter: 10 mm, thickness: 2 mm) and cultured at 37 °C for 48 h. During this period, the medium was replaced with fresh medium after 8, 16, and 24 h to culture biofilms. Then, the samples were stained with a LIVE/DEAD bacterial viability kit (Molecular Probes) and five sites were randomly selected under CLSM to analyses the biofilms on the resin surface. The biofilm thickness was measured using the Zen software (Carl Zeiss Microscopy) based on the vertical axis of the image. The average biomass was measured using the COMSTAT plug-in (Technical University of Denmark) along with ImageJ software (NIH).

To produce polished resin samples, resins with 3% PMEA-1 (disc-shaped, diameter: 10 mm, thicknesses: 2 mm) were polished using a SiC paper by 0.3 and 0.5 mm. The formation of human-saliva-derived biofilms was evaluated using the same procedure as that used for the other samples.

Aesthetics of fabricated occlusal splints

An experienced dental technician fabricated the occlusal splints.[40] Three identical gypsum models of a patient after orthodontic treatment were constructed. After setting the outline with wax, the mixture of resin was added over the outlined area to form the shape of the splints. Then, the resin was polymerized at 60 °C and 0.4 MPa for 15 min. The surface of the splint was smoothed and polished *via* a conventional method.[41] The surface gloss, direct transmittance, and color of the resins were measured using disc-shaped samples (n = 6) in accordance with a previous study.[40] An infrared gloss meter (IG-330) was used to measure the surface gloss, with the measurement angle set to 60°.[42] For each surface, we calculated the average value based on 6 different points. Direct transmittance (T%) was measured using an ultraviolet-visible (UV/vis) spectrophotometer (Lambda 20).[43] Measurements were performed in the wavelength range of 400–780 nm with a step size of 5 nm. The mean T% values at 525 nm were used to quantify the differences between the materials.

Statistical analysis

Statistical analysis was performed using IBM SPSS software (version 23.0; IBM Korea, Inc.). The results were analysed by one-way analysis of variance and *post-hoc* Tukey's tests. Statistical significance was set at $P < 0.05$.

Results

Denture base resins and materials design

In this study, we maximize the unique chemistry of denture resins to develop anti-fouling bulk materials with the required mechanical strength. In general, dentures are made of acrylic resins prepared by polymerizing a mixture of methyl methacrylate (MMA) monomer liquid and poly(methyl methacrylate) (PMMA) solid powder in a mold. The powder consists of micrometer-sized beads (20–60 μm) of PMMA. The MMA monomers penetrate and swell the surface of beads, and thus the beads release a part of the PMMA polymer chains from the bead surface.[44] The polymerizing PMMA chains form a physically entangled network with the polymer chains of microbeads (inter-penetrating network), and the resin sets before all beads are dissolved (Fig. 1).[45] Therefore, the denture resins are resin composites consisting of PMMA fillers embedded in the PMMA matrix, as PMMA fillers reduce the polymerization shrinkage as well as provide the mechanical strength. Because all components are PMMA, the resins show good appearance (transparency and surface gross), which requires for clinical use as a denture base. In our material design, the MMA liquid was used as a solvent to dissolve PMEA, and then mixed with a PMMA powder, followed by polymerization. This unique chemistry allows incorporation of PMEA in the PMMA matrix as well as fabrication to bulk materials with desired shapes (dentures) in a mold.

Polymer synthesis and characterization

Because PMEA is an oily polymer, its molecular size would affect the bulk and surface properties of resins because of the high mobility and MW-dependent miscibility with PMMA.[23] To that end, we synthesized a series of PMEA with a range of MWs by free-radical polymerization in the presence of a thinyl CTA to investigate the effect of MW on their properties. Low-MW polymers were prepared by increasing the ratio of CTA to monomer (Table 1). The PMEA samples synthesized with 10, 1, 0.1, and 0 mol% of CTA were denoted as PMEA-1, PMEA-2, PMEA-3, and PMEA-4, respectively. Different lots of the polymers prepared under the same condition is denoted as a small letter of "a" and "b" after the sample name. All the polymer samples were an oily or viscus liquid. The MW of PMEA-1 was 1200–1700 g mol^{-1} with relatively narrow MW distribution of $D < 1.6$ (Table 2), which was reproducible for 2 independent polymerizations. On the other hand, PMEA-4 samples, which prepared without CTA, have high MWs (>80 000 g mol^{-1}) and very broad MW distribution ($D > 3.5$). For comparison, MEA monomer was used instead of PMEA, which was covalently incorporated into the PMMA resin matrix as a mono-functional group.

Mechanical properties

It has been reported that the MW of PMEA affects its miscibility with PMMA.[23] To investigate the effect of the MW of PMEA on the resin properties, the mechanical properties of the resins containing the PMEA polymers with a range of molecular weights at various concentrations were evaluated. For comparison, MEA monomer was used instead of PMEA, which was covalently incorporated into the PMMA resin matrix as a mono-functional group. There were no differences between the mechanical properties of the control resin and the resins with PMEA-1 at up to 5 wt% (Fig. 2A–C and Tables S1–3†). The flexural strength and elastic modulus decreased at 10 wt% PMEA; however, the values were still higher than those recommended by the ISO standard. High-MW PMEA-4 resin had significantly lower values of the mechanical properties at low PMEA concentrations (3 wt%) than those of the control. The resin with MEA also retained these properties for higher MEA concentrations, except the flexural modulus, suggesting that the polymer properties of PMEA are responsible for degrading the mechanical properties of PMMA resins. Based on the mechanical properties, we selected the low-MW PMEA-1 and PMEA-4 resins at 3 wt% for further experiments.

The mechanical properties of the thermocycled resins were also examined. After the aging process, the flexural strengths of the control and PMEA-1 resins slightly decreased and reached the same values (Fig. 2D–F and Tables S4–6†); thus, this decrease is likely related to the inherent properties of the PMMA resin, rather than those of PMEA-1.

Morphological properties

SEM images showed that the fractured surfaces of the control and PMEA-1 resins were quite smooth and flat, although there was some protruding texture (Fig. 2G and Fig. S2†). In contrast, the fractured surface of PMEA-4 resin was very uneven and rough, including some pores, which may be responsible for the high turbidity of the resin.

Biocompatibility

The L929 cell viability of the PMEA-1 resin was reduced to 80% that of the blank sample; however, it still exceeded the requirement (70%) specified by the ISO standards (Fig. 2H). The PMEA has been reported to show adequate biocompatibility to human cells.[18–20] It has been known that the unreacted MMA monomer leach out from PMMA dental resins and cause cytotoxicity.[46] Because there was no statistically significant difference between the control and PMEA-1 resin, the observed cytotoxicity of the PMEA-1 resin likely due to the MMA leached from the PMMA resin, but not PMEA-1. In contrast, there was a significant decrease in the cell viability of the PMEA-4 resin. Because of poor mechanical properties and the presence of defects in the bulk structures, we speculate that PMEA-4 might significantly compromise the polymerization, and a substantial amount of unreacted MMA monomers remained in the resulted resin. The free MMA monomers might be released, thereby causing cytotoxicity.

Taken together, the resin with PMEA-1 meet the material requirements for clinical performance of dental denture resins in terms of the mechanical properties, longevity, aesthetics, and biocompatibility.

Bulk and surface PMEA distribution

Rhodamine-labeled PMEA-1 (PMEA-Rh) was incorporated into the resin. PMEA-1Rh was distributed throughout the resin structure (Fig. 3A), but some regions showed stronger fluorescence signals, indicating the aggregation or separation of PMEA-Rh. The observation of PMEA-Rh near the surface indicates that some fluorescence signals around PMMA microbeads (non-fluorescent circles) (Fig. 3A–C) were stronger than the miscible control PMMA-Rh (Fig. 3D). We speculate that PMEA-Rh accumulated on the surface of the original PMMA beads before dissolution.

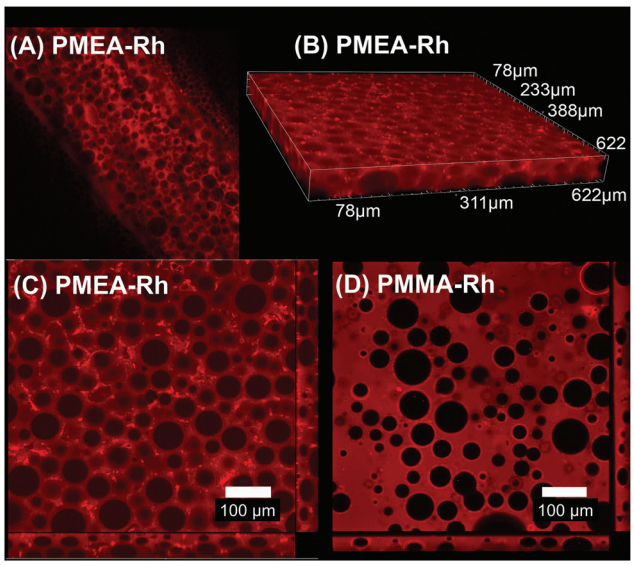

Fig. 3 Confocal fluorescence images of resins with fluorescent PMEA or PMMA: (A) vertical cross-section of PMEA-Rh resin with a thickness of 780 μm; (B) 3-dimensional image of PMEA-Rh resin near the surface; (C) surface of PMEA-Rh resin; (D) surface of PMMA-Rh resin. The "b-series" PMEA lots were used for PMEA distribution evaluation (Table 2).

Wettability

There was no statistically significant difference in the contact angle between the control and PMEA-1 resins. The PMEA-4 resin had the lowest contact angle value (83.8 ± 6.1°), indicating that the PMEA-4 resin surface is more hydrophilic. The PMEA-1 resin had a lower surface energy (32.13 ± 1.99 mN m^{-1}) compared to that of the control (39.74 ± 2.17 mN m^{-1}); the PMEA-4 resin possessed an even lower surface energy (26.6 ± 4.6 mN m^{-1}) (Fig. 4A). Although the PMEA-1 resin was not the most hydrophilic, it had the lowest contact angle hysteresis (36.0 ± 3.7°), indicating that the resin surface was more slippery compared to other resin surfaces.

Tribological performance

The coefficient of friction (COF) of the control and MEA resins monotonically increased until constant values of ~0.3 were reached after 200 cycles. Interestingly, the COF values of the PMEA-1 and PMEA-4 resins reached the maximum values of ~0.4 at around 50 cycles and decreased to ~0.3 at 1000 cycles, which was close to that of the control (Fig. 4C).

Protein adsorption

The PMEA-1 resin showed ~20% reduction in BSA adsorption compared to that of the control, while there was no statistically significant difference between the PMEA-1 and PMEA-4 resins (Fig. S3†). The PMEA-4 resin showed larger reduction in adsorption than PMEA-1, which appeared to reflect the contact angle value.

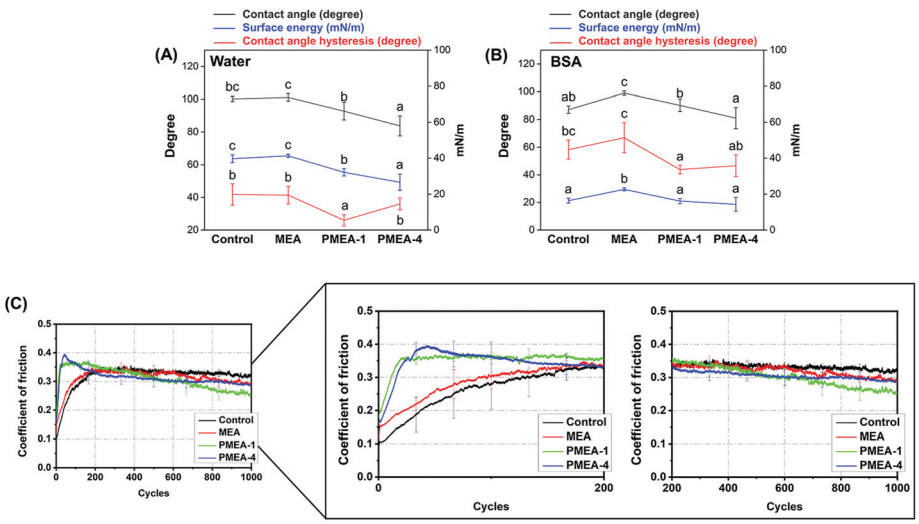

Fig. 4 Surface wettability and tribological performance. Contact angle, calculated surface energy, and contact angle hysteresis of resins measured with (A) distilled water or (B) 2 mg ml^{-1} BSA solution as a reference liquid. Alphabetical letters on the marks present statistical grouping ($a < b < c$, $p < 0.05$). (C) Coefficient of friction of resins as a function of loading cycles. The "b-series" PMEA lots were used for wettability and tribological evaluation (Table 2).

Bacterial and fungal attachment

Fluorescence and FE-SEM images show that there were significantly fewer *S. mutans* cells attached to the PMEA-1 resin than the control (Fig. 5A and C). There was no morphological change in the *S. mutans* cells attached to the surface (Fig. 5C), suggesting that the attached cells were still viable. Quantitative CFU analysis confirmed that the PMEA-1 resin had the least viable *S. mutans* adhesion (Fig. 5B) among the groups. Additionally, the resins were tested for the adhesion of *C. albicans* (Fig. 5D–F). Similar to *S. mutans*, the PMEA-1 resin reduced *C. albicans* attachment most significantly.

Saliva-derived biofilm

The thickness and biomass values of biofilms derived from human saliva on the PMEA-1 resin were ~50% lower than those for the control ($P < 0.001$), whereas the PMEA-4 resin values were only 20% lower (Fig. 6A–C, Tables S7 and S8†). The thickness and biomass of the resin with MEA were not significantly different from those of the control. There was also no significant difference between the pre- and post-aged biofilm thickness and biomass for all resin types (Fig. 6B and C). These results suggest that the resins effectively protect against the formation of human salivary biofilms and are highly stable.

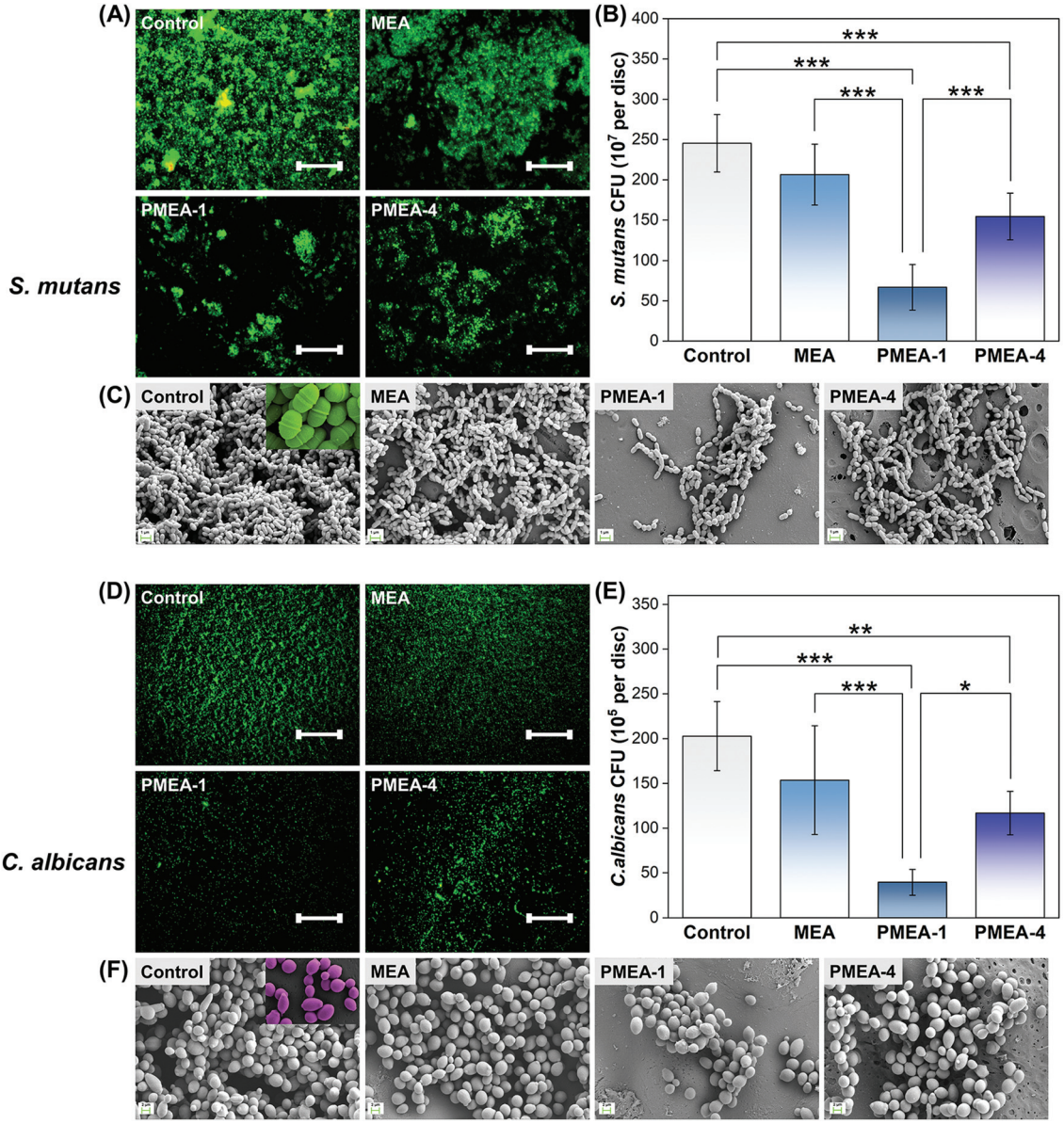

Fig. 5 Oral bacterial and fungal attachment to resin surfaces. Representative LIVE/DEAD staining images showing (A) *Streptococcus mutans* and (D) *Candida albicans* attachment to the resin surfaces. Scale bar is 500 μm. (B) *Streptococcus mutans* and (E) *Candida albicans* CFU counts on the surfaces of the resins; asterisks indicate statistical significance (* $P < 0.05$, ** $P < 0.01$, and *** $P < 0.001$). Representative SEM images of (C) *Streptococcus mutans* and (F) *Candida albicans* attached to the surfaces of the resins (magnification: 5000× and 2000×, respectively). The "b-series" PMEA lots were used for biological experiments (Table 2).

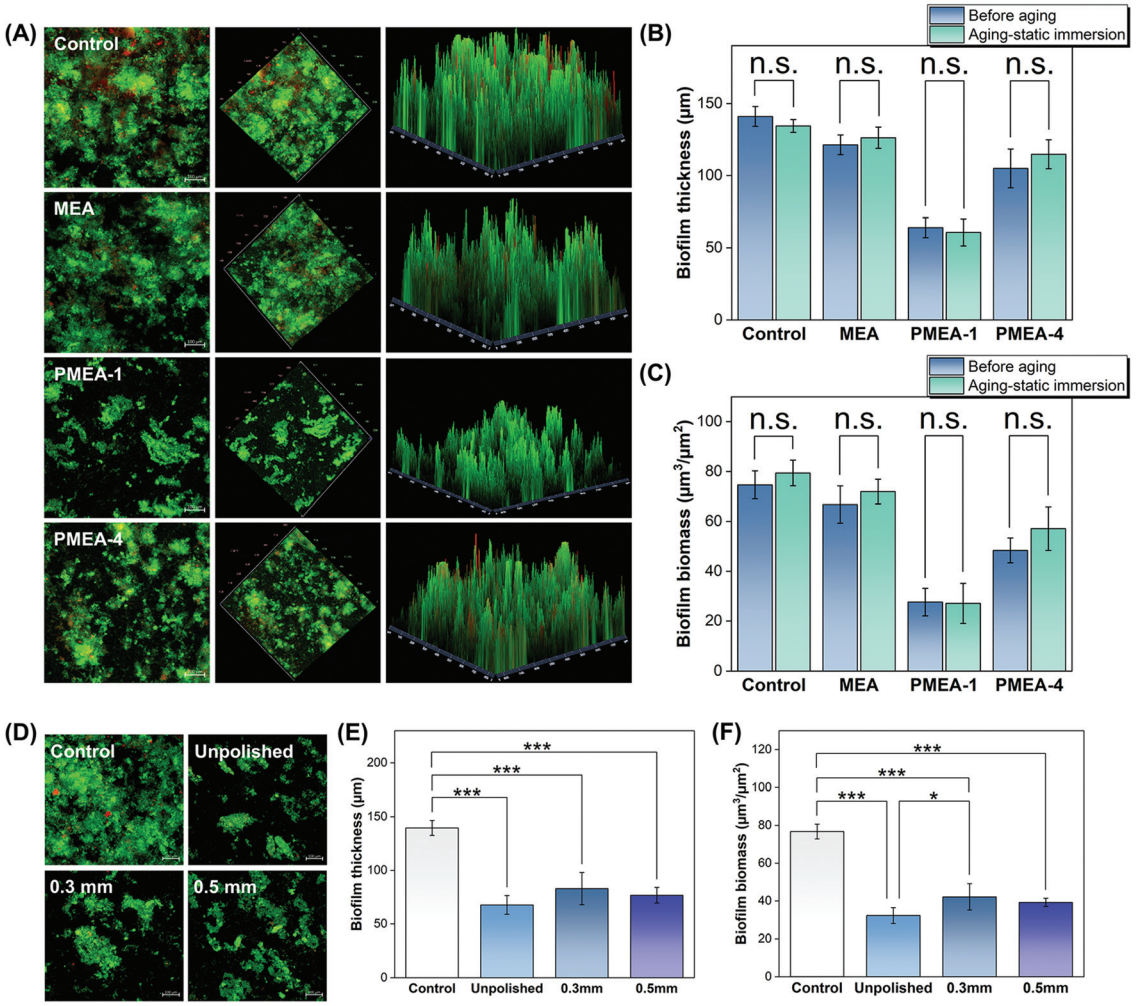

Fig. 6 Anti-biofilm performance of resins before and after the static immersion and polishing of PMEA resin surfaces. (A) Two- and three-dimensional images of LIVE/DEAD stained human-salivary-derived biofilms attached to the resin surfaces and their biofilm (B) thickness and (C) mass. Statistical comparisons due to static-immersion aging are detailed in Tables S7–8.† (D) LIVE/DEAD stained images of the human-salivary-derived biofilm attached to the unpolished and polished PMEA-1 resin surfaces. Influence of the polishing on biofilm (E) thickness and (F) mass. The "b-series" PMEA lots were used for biological experiments (Table 2). Asterisks indicate statistical significance (n.s.: not significant, * $P < 0.05$, and *** $P < 0.001$).

Polished surfaces

The surfaces of resins polished to a depth of 0.3 or 0.5 mm were tested for biofilm formation by salivary bacteria. Analysis of the fluorescence images indicated that the biofilm formation on the polished surfaces was less severe than that on the control, and the polished and unpolished surfaces had similar anti-biofilm performance considering the biofilm mass and thickness (Fig. 6D–F).

Aesthetics of fabricated occlusal splints

The resin with PMEA-1 showed no significant difference compared to the control resin, which has been used for denture fabrication (Fig. 7A). There was no significant difference in surface gloss and direct transmittance between the 3 wt% PMEA-1 resin and control resin, while the direct transmittance of the PMEA-4 resin was significantly lower (Fig. 7B and C).

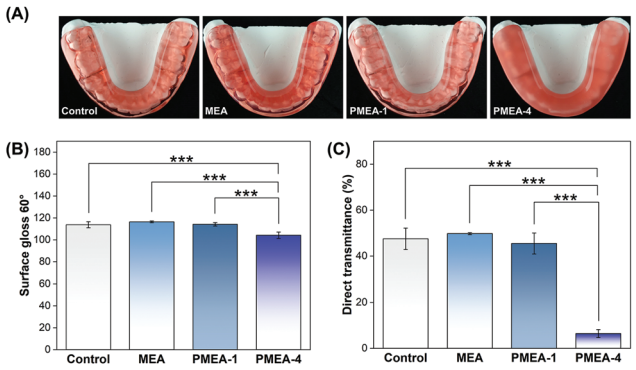

Fig. 7 (A) Actual occlusal splints fabricated using the materials. (B) Surface gloss and (C) direct transmittance of resins with or without PMEA; asterisks indicate statistical significance (*** $P < 0.001$). The "b-series" PMEA lots were used for occlusal splints fabrication (Table 2).

Discussion

In our material design, PMEA was first dissolved into the MMA liquid and then mixed with PMMA powder, followed by polymerization. The unique chemistry of this denture base resin enables incorporation of PMEA into the PMMA matrix and the fabrication of desired shapes (dentures) by molding. This differs from the conventional method for polymer films in which PMEA and PMMA polymers are dissolved in an organic co-solvent and cast on substrates, followed by evaporation and annealing.[25] It has been previously demonstrated that PMEA migrates to the surface of a PMMA film after annealing at high temperatures above the glass transition temperature (T_g) of the polymers. However, our resin with PMEA-1 did not show any surface segregation (Fig. 3), likely due to the low MW and low concentration (3 wt%) of PMEA, which resulted in good miscibility with PMMA.[23] In addition, the PMEA polymer chains could be trapped in the glassy PMMA matrix during the polymerization because the polymerization temperature is lower than the T_g of PMMA. Nevertheless, the effective distribution of PMEA in the resin is advantageous for the anti-fouling performance of polished or scratched resin surfaces, without degrading the mechanical proprieties and aesthetics.

The mechanical properties of the resins are important criteria for clinical use of denture base materials that are subject to a large biting force and repeated mechanical loads in the oral cavity. To that end, we first tested a series of PMEA with a range of MW in different concentrations for their flexural strength, elastic modulus, and Vickers microhardness. In general, the mechanical properties of the control resin were retained for low-MW PMEA at low concentrations. The oily state of PMEA (T_g = −50 °C) could be responsible for the reduced mechanical properties at high concentrations. High-MW PMEA-4 showed significantly reduced values at low PMEA concentrations, which may be due to the local formation of PMEA-4 soft domains in the PMMA matrix, and possibly the low conversion of MMA during polymerization. In addition, dentures undergo many temperature cycles in their use, which may cause mechanical degradation. Therefore, it is important to evaluate the effect of thermal aging on their properties. The results showed that PMEA-1 did not degrade the mechanical properties of dental resins after aging treatment, supporting the clinical longevity of the resins.

The aesthetics of denture resins is a very important factor for their clinical use, which, for example, should mimic the appearance of oral tissues. The resin with PMEA-1 showed no significant difference compared to the control resin, which has been used for denture fabrication, both with respect to the surface gloss and direct transmittance. This suggests that PMEA-1 does not alter the standard PMMA resin appearance and thus can be used for dental applications. Indeed, there was no apparent difference in model occlusal splints between the control and resin with PMEA-1 (Fig. 7A). It should be noted that the pink color was due to a pigment in the commercial product. In contrast, the direct transmittance of the resin with PMEA-4 was significantly less than that of the control, which caused undesired high turbidity in the occlusal splint. This is likely due to the rough structure of the bulk as the SEM image (Fig. 2G) indicated.

The cytotoxicity results showed that there was no statistically significant difference in the cell viability between the control and resin with PMEA-1, indicating that there was no significant leaching of toxic monomers. In contrast, the resin with PMEA-4 showed a significant reduction in the cell viability. Because of the poor mechanical properties and defects in the bulk structures, we speculate that polymerization of the PMEA-4 sample may have been limited, and thus the resulting resin released a substantial amount of free unreacted MMA, resulting in cytotoxicity. Taken together, the PMEA-1 resin had mechanical, longevity, aesthetics, and biocompatibility properties that meet the material requirements for clinical application of dental denture resins.

The PMEA-1 resin was also effective in reducing the formation of biofilms by *S. mutans*, *C. albicans*, and salivary bacteria. The pre- and post-aged PMEA-1 resins showed the same level of anti-fouling activity, indicating that the resins were highly stable. This stability can be attributed to the low water solubility of PMEA, as well as the glassy PMMA matrix capturing PMEA, which effectively prevents PMEA leaching. The denture surface is frequently scratched and abraded by food, oral tissue, and cleaning brushes, which would compromise the anti-fouling activity of the resin surface, particular those with polymer coatings. Polishing of the PMEA-1 resin surface did not alter the anti-biofilm activity of the resin because the PMEA polymers in the matrix were exposed and were present on the polished surface. This result suggests that scratched dentures would be able to effectively prevent microbial attachment during use, and fabricated dentures after polishing would have antimicrobial activity without further modification. Thus, our approach is practical for clinical use and compatible with the current denture fabrication procedure.

Our results indicated that PMEA-1 reduced microbial attachment substantially. In general, anti-fouling polymers and coatings are expected to act directly to repel protein and microbes, but 3 wt% of PMEA-1 would be too low to cover and protect the entire surface area. Therefore, it is unclear how such a small quantity of polymer could form an anti-fouling surface. It has been reported that PMMA polymer chains at the water interface have high chain mobility although the PMMA bulk is glassy (T_g = ∼100 °C).[25] We hypothesize that the PMEA additive increased the surface chain mobility of the resin surface. The rubbery states of PMEA could contribute to loosening the tight packing of glassy PMMA chains and swelling, thus increasing the chain mobility of surface polymers. The tribological results showed that the PMMA matrix with PMEA was worn out first. Because the friction coefficient of the resin with MEA, which was covalently incorporated into the matrix, showed similar behavior to that of the control, the free polymer chains of PMEA are likely responsible for the high friction. Therefore, we propose that the high viscosity of PMEA polymer chains in the matrix increased the surface friction

and thus made the surface sticky. Once the matrix at the resin surface was worn out, the exposed PMMA microbeads were the dominant surface structure, and therefore, the friction coefficients of all samples reached similar values. This result can be explained by the surface mobility of PMEA. The high friction surface indicates that the resin surface contained highly mobile oily PMEA polymer chains, which increase the homogeneity of the surface microstructure and reduce kinetic barriers. In general, contact angle hysteresis is caused by heterogeneous surface microstructures and high kinetic barriers of solid surfaces for sliding.[47]

Previous studies demonstrated that polymer surface hydration plays an important role in preventing protein and microbial attachment.[48–51] However, the anti-biofilm activity of the resins appeared to be correlated to the contact angle hysteresis (slippery surface) rather than the contact angle or surface energy (*i.e.*, the hydrophilicity). This contrasts with the BSA adsorption, which is directly related to the contact angle and surface energy of the resin surfaces (Fig. 3S†). Previous studies demonstrated that impregnated lubricants, such as silicone oil, create slippery surfaces in resin, effective in preventing marine fouling.[52,53] The contact angle hysteresis and anti-fouling activity of polymer coatings is correlated.[47] Our results are in good agreement with those of this previous study. The tribological results also suggested that the resin surface contains PMEA polymer chains. We propose that the high mobility of oily PMEA polymer chains contributed to increasing the homogeneity of the surface microstructure and weakening the kinetic barriers. The high chain mobility of PMEA generates dynamic surfaces with low contact angle hysteresis values[47] unless the surface is not subjected to any mechanical loading. Because microbial attachment is a dynamic and concerted process, the slippery surface may disturb the attachment mechanism and/or facilitate the removal of attached bacteria, consequently inhibiting biofilm formation.

Conclusions

This study addressed the inherent challenges in the field of developing additives for anti-fouling dental resins with regards to their clinical performance and processing practicality. We demonstrated that the low-MW PMEA additive was able to generate a robust and biocompatible anti-fouling surface, but retained the mechanical properties and aesthetic appearance of dental PMMA resins. After aging treatments, the resins maintained their mechanical properties and anti-fouling activity, verifying the durability and longevity of this new material for clinical use. The polished surfaces showed the same level of reduction of oral biofilm formation, suggesting that while subject to constant scratching and abrasion by food and brushing, aged dentures would still be effective in preventing microbial attachment, and this new material would not require any surface retreatment or coating replenishment to regain anti-fouling performance. We propose that the PMEA additive acts by creating a slippery surface for microbes to prevent biofilm formation.

The proposed resin preparation is very practical and advantageous because the conventional materials, procedures, and equipment in the dental lab can be used for denture fabrication. In future work, the long-term microbial behaviors on the resins should be investigated to support the feasibility of our new materials for potential clinical translation. In addition, we also envision that *in vivo* evaluation would be part of our future research.

Author contributions

Jie Jin: conceptualization, methodology, data curation, validation, formal analysis, investigation, visualization, writing – original draft, writing – review & editing; Rajani Bhat, Utkarsh Mangal and Ji-Young Seo: investigation, methodology, validation; YouJin Min, Jaehun Yu, and Dae-Eun Kim: investigation, methodology; Kenichi Kuroda, Jae-Sung Kwon, and Sung-Hwan Choi: conceptualization, funding acquisition, project administration, resources, supervision, writing – review & editing. All authors revised the manuscript and approved the final manuscript.

Conflicts of interest

A patent application (Korean patent application no. 10-2021-0020380) has been filed.

Acknowledgements

This work was supported by a Korea Medical Device Development Fund grant provided by the Ministry of Science and ICT, the Ministry of Trade, Industry and Energy, the Ministry of Health and Welfare, the Ministry of Food and Drug Safety of Korea (Project Number: KMDF_PR_20200901_0067-01), and a National Research Foundation (NRF) of Korea grant funded by the Korean government (MSIT) (No. 2021R1A2C2091260). This work is also supported by the Department of Biologic and Materials Sciences & Prosthodontics, the University of Michigan School of Dentistry, and the University of Michigan Office of Research.

References

1 J. L. Ferracane, *J. Dent. Res.*, 2017, **96**, 364–371.
2 Y. Hao, X. Huang, X. Zhou, M. Li, B. Ren, X. Peng and L. Cheng, *Int. J. Mol. Sci.*, 2018, **19**, 3157.
3 H. Koo, R. N. Allan, R. P. Howlin, P. Stoodley and L. Hall-Stoodley, *Nat. Rev. Microbiol.*, 2017, **15**, 740–755.
4 J. Kreth, J. L. Ferracane, C. S. Pfeifer, S. Khajotia and J. Merritt, *J. Dent. Res.*, 2019, **98**, 850–852.

5 J. Kreth, J. Merritt, C. S. Pfeifer, S. Khajotia and J. L. Ferracane, *J. Dent. Res.*, 2020, **99**, 1140–1149.
6 R. J. Lamont, H. Koo and G. Hajishengallis, *Nat. Rev. Microbiol.*, 2018, **16**, 745–759.
7 N. J. Lin, *Dent. Mater.*, 2017, **33**, 667–680.
8 C. J. Nobile and A. D. Johnson, in *Annual Review of Microbiology, Vol 69*, ed. S. Gottesman, 2015, vol. 69, pp. 71–92.
9 T. Vila, A. S. Sultan, D. Montelongo-Jauregui and M. A. Jabra-Rizk, *J. Fungi*, 2020, **6**, 15.
10 T. Yoneyama, M. Yoshida, T. Matsui and H. Sasaki, *Lancet*, 1999, **354**, 515.
11 L. Gendreau and Z. G. Loewy, *J. Prosthodontics*, 2011, **20**, 251–260.
12 A. Yarborough, L. Cooper, I. Duqum, G. Mendonça, K. McGraw and L. Stoner, *J. Prosthodontics*, 2016, **25**, 288–301.
13 W. Choi, J. Jin, S. Park, J. Y. Kim, M. J. Lee, H. Sun, J. S. Kwon, H. Lee, S. H. Choi and J. Hong, *ACS Appl. Mater. Interfaces*, 2020, **12**, 7951–7965.
14 X. J. Lin, M. O. Boit, K. Wu, P. Jain, E. J. Liu, Y. F. Hsieh, Q. Zhou, B. W. Li, H. C. Hung and S. Y. Jiang, *Acta Biomater.*, 2020, **109**, 51–60.
15 L. Mi and S. Y. Jiang, *Angew. Chem., Int. Ed.*, 2014, **53**, 1746–1754.
16 L. Torres, Jr. and D. R. Bienek, *J. Funct. Biomater.*, 2020, **11**, 54.
17 J. S. Kwon, J. Y. Kim, U. Mangal, J. Y. Seo, M. J. Lee, J. Jin, J. H. Yu and S. H. Choi, *Int. J. Mol. Sci.*, 2021, **22**, 13.
18 C. Sato, M. Aoki and M. Tanaka, *Colloids Surf., B*, 2016, **145**, 586–596.
19 R. Koguchi, K. Jankova, N. Tanabe, Y. Amino, Y. Hayasaka, D. Kobayashi, T. Miyajima, K. Yamamoto and M. Tanaka, *Biomacromolecules*, 2019, **20**, 2265–2275.
20 M. Tanaka, S. Kobayashi, D. Murakami, F. Aratsu, A. Kashiwazaki, T. Hoshiba and K. Fukushima, *Bull. Chem. Soc. Jpn.*, 2019, **92**, 2043–2057.
21 T. Hirata, H. Matsuno, D. Kawaguchi, N. L. Yamada, M. Tanaka and K. Tanaka, *Polymer*, 2015, **78**, 219–224.
22 T. Hirata, H. Matsuno, D. Kawaguchi, N. L. Yamada, M. Tanaka and K. Tanaka, *Phys. Chem. Chem. Phys.*, 2015, **17**, 17399–17405.
23 T. Hirata, H. Matsuno, M. Tanaka and K. Tanaka, *Phys. Chem. Chem. Phys.*, 2011, **13**, 4928–4934.
24 T. Hirata, H. Matsuno, D. Kawaguchi, T. Hirai, N. L. Yamada, M. Tanaka and K. Tanaka, *Langmuir*, 2015, **31**, 3661–3667.
25 H. Aoki, R. Sekine, T. Iwamoto and S. Ito, *Polym. J.*, 2009, **42**, 124–130.
26 D. Murakami, N. Mawatari, T. Sonoda, A. Kashiwazaki and M. Tanaka, *Langmuir*, 2019, **35**, 2808–2813.
27 R. Koguchi, K. Jankova, Y. Hayasaka, D. Kobayashi, Y. Amino, T. Miyajima, S. Kobayashi, D. Murakami, K. Yamamoto and M. Tanaka, *ACS Biomater. Sci. Eng.*, 2020, **6**, 2855–2866.
28 Y. Toyokawa, S. Kobayashi, H. Tsuchiya, T. Shibuya, M. Aoki, J. Sumiya, S. Ooyama, T. Ishizawa, N. Makino, Y. Ueno and M. Tanaka, *Mater. Sci. Eng., C*, 2021, **120**, 111386.
29 ISO, ISO 20795-2:2010, 2010.
30 S. H. Choi, W. S. Jeong, J. Y. Cha, J. H. Lee, K. J. Lee, H. S. Yu, E. H. Choi, K. M. Kim and C. J. Hwang, *Dent. Mater.*, 2017, **33**, 1426–1435.
31 J. H. Lee, A. El-Fiqi, J. K. Jo, D. A. Kim, S. C. Kim, S. K. Jun, H. W. Kim and H. H. Lee, *Dent. Mater.*, 2016, **32**, 1564–1574.
32 U. Mangal, J. Y. Kim, J. Y. Seo, J. S. Kwon and S. H. Choi, *Materials*, 2019, **12**, 3438.
33 M. S. Gale and B. W. Darvell, *J. Dent.*, 1999, **27**, 89–99.
34 ISO, ISO 10993-5:2008, 2008.
35 ISO, ISO 10993-12:2012, 2012.
36 M. J. Lee, J. Y. Kim, J. Y. Seo, U. Mangal, J. Y. Cha, J. S. Kwon and S. H. Choi, *Nanomaterials*, 2020, **10**, 1581.
37 Z. Xu, X. Zhao, X. Chen, Z. Chen and Z. Xia, *RSC Adv.*, 2017, **7**, 52266–52273.
38 M. J. Lee, J. S. Kwon, J. Y. Kim, J. H. Ryu, J. Y. Seo, S. Jang, K. M. Kim, C. J. Hwang and S. H. Choi, *Dent. Mater.*, 2019, **35**, 1331–1341.
39 J. S. Kwon, M. J. Lee, J. Y. Kim, D. Kim, J. H. Ryu, S. Jang, K. M. Kim, C. J. Hwang and S. H. Choi, *Sci. Rep.*, 2019, **9**, 1432.
40 J. Jin, J.-Y. Kim, W. Choi, M.-J. Lee, J.-Y. Seo, J. Yu, J.-S. Kwon, J. Hong and S.-H. Choi, *J. Ind. Eng. Chem.*, 2020, **86**, 194–204.
41 C. A. Kass and J. N. Tregaskes, *J. Prosthet. Dent.*, 1978, **40**, 461–463.
42 A. Kakaboura, M. Fragouli, C. Rahiotis and N. Silikas, *J. Mater. Sci. Mater. Med.*, 2007, **18**, 155–163.
43 A. Della Bona, A. D. Nogueira and O. E. Pecho, *J. Dent.*, 2014, **42**, 1202–1209.
44 M. S. Zafar, *Polymers*, 2020, **12**, 2299.
45 P. K. Vallittu, *J. Adhes. Sci. Technol.*, 2009, **23**, 961–972.
46 C. Bural, E. Aktaş, G. Deniz, Y. Ünlüçerçi, N. Kızılcan and G. Bayraktar, *Dent. Mater.*, 2011, **27**, 1135–1143.
47 D. L. Schmidt, R. F. Brady, K. Lam, D. C. Schmidt and M. K. Chaudhury, *Langmuir*, 2004, **20**, 2830–2836.
48 W. F. Lin and J. Klein, *Curr. Opin. Colloid Interface Sci.*, 2019, **44**, 94–106.
49 Y. Zhang, Y. Liu, B. Ren, D. Zhang, S. Xie, Y. Chang, J. Yang, J. Wu, L. Xu and J. Zheng, *J. Phys. D: Appl. Phys.*, 2019, **52**, 403001.
50 M. A. Bag and L. M. Valenzuela, *Int. J. Mol. Sci.*, 2017, **18**, 1422.
51 W. J. Yang, K. G. Neoh, E. T. Kang, S. L. M. Teo and D. Rittschof, *Prog. Polym. Sci.*, 2014, **39**, 1017–1042.
52 H. Zhao, Q. Sun, X. Deng and J. Cui, *Adv. Mater.*, 2018, e1802141, DOI: **10.1002/adma.201802141**.
53 H. Jin, T. Zhang, W. Bing, S. Dong and L. Tian, *J. Mater. Chem. B*, 2019, **7**, 488–497.